ChemComm

One-step topochemical transformation of MoAlB into metastable Mo2AlB2 using a metal chloride salt reaction

Journal:	*ChemComm*
Manuscript ID	CC-COM-01-2023-000138.R1
Article Type:	Communication

COMMUNICATION

One-step topochemical transformation of MoAlB into metastable Mo_2AlB_2 using a metal chloride salt reaction

Received 00th January 20xx,
Accepted 00th January 20xx

DOI: 10.1039/x0xx00000x

Katelyn J. Baumler,[a] Owen S. Adams,[a] and Raymond E. Schaak*[a,b,c]

Reacting MoAlB with $ZnCl_2$ at 550 °C produces metastable Mo_2AlB_2 through a one-step topochemical transformation. This reaction showcases differences in reactivity between boride-based MAB phases and carbide-based MAX phases, which are solid-state precursors to an important family of 2-D materials.

MAX phases comprise an important family of layered solid-state compounds that have revolutionized the fabrication of two-dimensional (2-D) metal carbide nanosheets, which have diverse applications spanning energy conversion and storage, catalysis, optics, electronics, sensing, electromagnetics, environmental remediation, medicine, and structural composites.[1,2] In a MAX phase, where M is a transition metal, A is a light p-block element such as aluminum, and X is carbon or nitrogen, M-X layers alternate with A layers. The bonding between the A layers and M elements is much weaker than the covalent bonding within the M-X layers, allowing A to be selectively targeted for topochemical manipulations that modify composition while preserving crystal structure.[2] For example, the A element can be removed from MAX phases to form 2-D M-X nanosheets that are called MXenes, as is typified by the reaction of Ti_3AlC_2 with aqueous HF to form 2-D $Ti_3C_2T_x$ (T = terminating group). The A element can also be replaced, as has been shown for the reaction of Ti_3AlC_2 with the Lewis acid $ZnCl_2$ to form isostructural Ti_3ZnC_2.[3]

MAB phases and MBenes, which are boride analogues of MAX phases and MXenes, have emerged as potentially powerful alternatives to their carbide and nitride counterparts. MBenes, in particular, are poised to have unique properties and applications relative to MXenes, including as anodes for Li, Na, and Mg ion batteries[4–7] and as catalysts for the hydrogen evolution, oxygen evolution, nitrogen reduction, and CO_2 reduction reactions.[8–10] However, the synthesis of MBenes lags far behind that of MXenes, and this limitation is due, in part, to the unique chemical and structural characteristics of MAB phases. First, the M-B layers of MAB phases are prone to etching and corrosion in HF, which is the most common A-element etchant, while HF preserves the M-X layers of MAX phases.[11] Second, common MAB phases, such as MoAlB, have a double layer of the A element between M-B layers, while most MAX phases have only a single layer. Third, the Mo-Al bond in MoAlB, which has a double layer of Al, was found to be stronger than in Mo_2AlB_2, which has a single layer of Al.[4] This is important because the difference in Mo-Al bond strength makes Mo_2AlB_2, a metastable phase that is not easily synthesized, a better precursor to a MBene than MoAlB, a stable and synthetically tractable phase.[12] As a useful metastable compound, Mo_2AlB_2 is therefore an interesting and important synthetic target that represents a more general and fundamental challenge – how to rationally synthesize, in high yield, a metastable metal boride in a refractory system where direct high-temperature solid-state synthesis is too energetic.

Because it is metastable, Mo_2AlB_2 has been studied computationally more than it has been studied experimentally. A Mo_2AlB_2-like compound was synthesized by reacting MoAlB with 3 M LiF and 10 M HCl at 40 °C; the XRD pattern for this product approaches that of Mo_2AlB_2 but has significant $MoAl_{1-x}B$ character, suggesting incomplete Al extraction and/or incomplete crystallization.[13] [Note that MoAlB is equivalent to "$Mo_2Al_2B_2$" and that formation of Mo_2AlB_2 requires removing one Al from "$Mo_2Al_2B_2$", or half of the Al from MoAlB, *i.e.*, $MoAl_{0.5}B$.] Complete removal of a half equivalent of Al from MoAlB and formation of crystalline Mo_2AlB_2 was achieved upon gentle heating of $MoAl_{1-x}B$ (formed by aqueous NaOH treatment of MoAlB), which expelled residual Al as alumina and allowed the metastable phase to crystallize.[14] This process is diffusion controlled and therefore requires a laborious multi-step size selection process to isolate submicron grains of MoAlB

[a] Department of Chemistry, The Pennsylvania State University, University Park, PA, 16802, USA.
[b] Department of Chemical Engineering, The Pennsylvania State University, University Park, PA, 16802, USA.
[c] Materials Research Institute, The Pennsylvania State University, University Park, PA, 16802, USA.
Electronic Supplementary Information (ESI) available: Experimental details and additional XRD and SEM-EDS data. See DOI: 10.1039/x0xx00000x

before the subsequent low-temperature chemical and thermal treatments are applied.

Here, we report a one-step topochemical reaction that directly transforms MoAlB into metastable Mo_2AlB_2. We show that crystalline Mo_2AlB_2 forms from the reaction of MoAlB with $ZnCl_2$ at 550 °C for 170 h and elucidate key details of how the reaction proceeds and is driven. This reaction is comparable to the replacement reaction used to transform Ti_3AlC_2 to Ti_3ZnC_2,[3] as mentioned above, which highlights an important difference in reactivity and product formation between carbide-based MAX phases and boride-based MAB phases.

Before describing the reaction of the MAB phase MoAlB with $ZnCl_2$, it is helpful to consider more details of the reaction between carbide-based MAX phases and Lewis acid salts. Ti_3AlC_2 reacts with a near-stoichiometric amount of $ZnCl_2$ at 550 °C for 5 hours to form Ti_3ZnC_2, where Zn replaces Al.[3] The proposed pathway involves oxidation of Al to Al^{3+} and concomitant reduction of Zn^{2+} to Zn. In the presence of a significant excess of $ZnCl_2$, that same reaction was reported to expel zinc and produce exfoliated Cl-terminated $Ti_3C_2Cl_2$ sheets.[3] This method was further generalized to show that various metal chloride salts can be used, as long as the redox pair is favorable, and that it was possible to etch out different A elements including Zn, Si, and Ga.[15] In contrast to the MAX phases, we find that a comparable reaction between $ZnCl_2$ and the MAB phase MoAlB behaves differently and forms a different type of product.

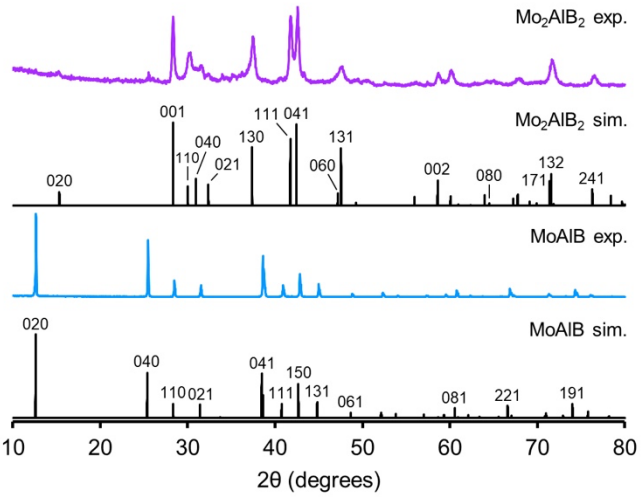

Figure 1. Powder XRD patterns for MoAlB (blue) and Mo_2AlB_2 (purple) formed upon reacting MoAlB with $ZnCl_2$ at 550 °C for 170 h. Reference patterns for MoAlB[16] and Mo_2AlB_2[14], incorporating preferred orientation as described in the ESI, are shown for comparison.

MoAlB was synthesized by heating MoB powder and Al chips to 1400 °C under flowing Ar for 10 h, followed by decreasing the temperature to 900 °C at 60 °C/h and then quickly cooling to room temperature.[14] The MoAlB product was crushed to a powder with a mortar and pestle and then placed in a porcelain boat. $ZnCl_2$ powder was added on top of the MoAlB powder in a 1:10 MoAlB:$ZnCl_2$ ratio. This mixture was then heated to 550 °C under flowing nitrogen for 170 h to ensure a complete reaction, cooled to room temperature, washed with water to remove any remaining $ZnCl_2$, and dried under ambient conditions.

Figure 1 shows a powder X-ray diffraction (XRD) pattern for as-synthesized MoAlB. The XRD pattern matches well with the simulated XRD pattern based on published crystallographic data[16] and the incorporation of preferred orientation based on the enhanced intensities of the 0*k*0 family of planes (Figure S1), which is consistent with the known crystal growth behavior of the layered MoAlB compound as plates.[11] Figure 1 also shows the XRD pattern for the product of the reaction between MoAlB and $ZnCl_2$ at 550 °C for 170 h. The experimental XRD pattern matches well with the simulated pattern for Mo_2AlB_2[14] with preferred orientation (Figure S1), though there is also evidence of small ZnO and Al_2O_3 impurities (Figure S2). The large shift in the lowest-angle peak, from 12.6 °2θ in MoAlB to 15.3 °2θ in Mo_2AlB_2, is especially diagnostic, as it is located exactly where it is expected for Mo_2AlB_2 and is consistent with complete removal of half of the Al in MoAlB. The sharpness of the peaks in the XRD pattern of Mo_2AlB_2, particularly the (111) and (041) reflections that can be resolved, exceeds that of prior reports and points to the high crystallinity of the compound. Also, it is known that MoAlB transforms to Mo_2AlB_2 through the formation and coalescence of stacking faults that emerge from removing half of the double layer of Al that separates the Mo-B layers, ultimately forming a single Al layer (Figure 2).[14] This formation of stacking faults and the concomitant structural disorder in *h*00 causes a minor suppression and broadening of the *hkl* peaks with nonzero *h* values; a detailed explanation, with accompanying reference XRD pattern, is included in the ESI.

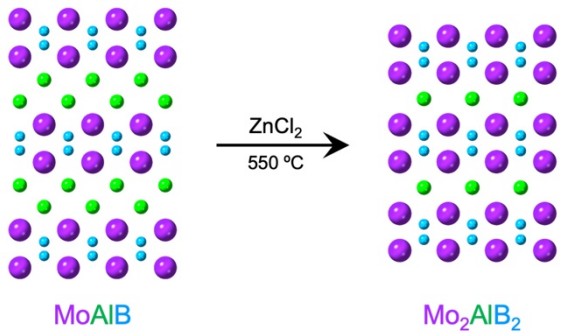

Figure 2. $ZnCl_2$-mediated reaction that converts MoAlB, which has a double layer of Al between Mo-B layers, to Mo_2AlB_2, which contains only a single Al layer.

Figure 3a shows an SEM image of the Mo_2AlB_2 product. The powder consists of nonuniform grains having various sizes, ranging from approx. 1 – 30 μm; the platelet morphology is evident for some grains, based on their orientation (Figure 3b). The corresponding SEM-EDS element maps showing Mo, Al, and Zn signals confirm that Mo and Al are co-localized throughout the Mo_2AlB_2 powder. A few small regions of brighter Al and Zn signal are present and are attributable to alumina and zinc oxide, respectively. Consistent with this observation, small amounts of ZnO and Al_2O_3 were observed in the XRD pattern in Figure 1. The EDS spectrum in Figure 3c confirms the 2:1 Mo:Al ratio in the Mo_2AlB_2 product while also validating that only a small amount of Zn (as ZnO) is present; additional data are provided in Figure S3. This result indicates that Mo_2AlB_2 forms instead of Mo_2ZnB_2 or MoZnB, which would be the Zn exchange products that could be expected based on the outcome of the

analogous $ZnCl_2$ reaction applied to carbide-based MAX phase Ti_3AlC_2.

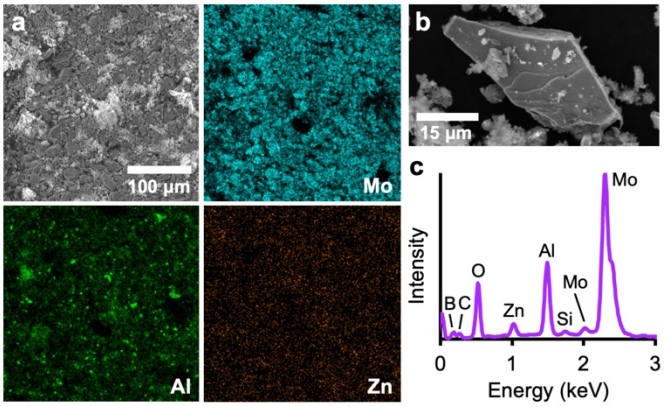

Figure 3. (a) SEM and SEM-EDS images of the surface of a pressed pellet of Mo_2AlB_2 formed from reacting MoAlB with $ZnCl_2$ at 550 °C. (b) SEM image of a plate shaped Mo_2AlB_2 crystallite. (c) EDS spectrum corresponding to sample in (a), showing that only a small amount of Zn remains and that the Mo:Al ratio is 2:1.

The formation of Mo_2AlB_2 instead of Zn exchange products highlights the different reactivity that occurs for MAB *vs*. MAX phases. The reaction times are also different. While the reaction of Ti_3AlC_2 with $ZnCl_2$ to form Ti_3ZnC_2 (or $Ti_3C_2Cl_2$) requires only 5 h at 550 °C, the reaction of MoAlB with $ZnCl_2$ at 550 °C to form Mo_2AlB_2 requires 170 h to reach completion. This difference in reaction time can be rationalized based on the differences in the interlayer M-A bond strengths. The M-A bond strengths in MAX phases, such as V_2AlC, are similar to that in Mo_2AlB_2. V_2AlC is also easier to etch the interlayer Al than MoAlB, which suggests that Mo_2AlB_2 should be easier to etch than MoAlB.[4]

To gain insights into the chemistry that drives the transformation of MoAlB into Mo_2AlB_2 upon reaction with $ZnCl_2$, we considered complementary reactions under the same conditions but using different metal salts. The reaction of the carbide-based MAX phase Ti_3AlC_2 with $ZnCl_2$ is understood as a redox pathway that involves the oxidation of Al to Al^{3+} concomitant with the reduction of Zn^{2+} to Zn. Such a reaction is consistent with general trends in standard reduction potentials, where Al would be more prone to oxidation while Zn would be more prone to reduction. To probe the role of redox chemistry, we chose to study the reaction of MoAlB with another metal salt, $NiCl_2$, that would exhibit similar redox behavior with Al as $ZnCl_2$, as well as with NaCl and LiCl, which are two salts with metals that would not be expected to be redox active with Al. We also chose a temperature of 650 °C for this set of reactions to further interrogate the effects of the reaction occurring in the liquid *vs*. the solid states, as $ZnCl_2$ and LiCl melt below 650 °C while $NiCl_2$ and NaCl melt above 650 °C. ($ZnCl_2$ is also molten at 550 °C where the initial reaction is carried out.) Finally, we chose to have the reactions only proceed for 1 h, both because of the higher temperature (650 °C *vs.* 550 °C) and because shorter reaction times can reveal insights into intermediates or byproducts that may form prior to the reaction reaching completion.

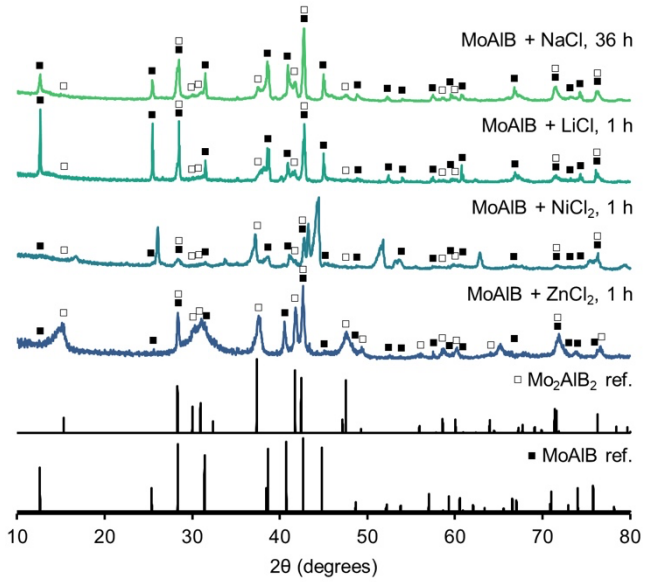

Figure 4. Powder XRD patterns for the products of reactions of MoAlB with four metal chloride salts. Reference pattern for MoAlB[16] and Mo_2AlB_2[14] are shown for comparison. MoAlB (■) and Mo_2AlB_2 (□) are present, in varying amounts, in each pattern.

Figure 4 (enlarged in Figure S4) shows XRD data for the products of these reactions. $ZnCl_2$, representing a good redox pair with Al that melts below 650 °C, shows evidence of Mo_2AlB_2 formation, and therefore of Al removal, within 1 h. $NiCl_2$, representing a good redox pair with Al that remains as a solid at 650 °C, also shows evidence of Mo_2AlB_2 formation, along with some residual unreacted MoAlB and some Ni- and Mo-containing decomposition products, which are expected given the higher reaction temperature (Figure S5). The fraction of Mo_2AlB_2 formed in the $NiCl_2$ sample is much lower than in the $ZnCl_2$ sample, which is consistent with the solid-state $NiCl_2$ reaction occurring slower than the liquid-state $ZnCl_2$ reaction. LiCl, which represents a bad redox pair with Al that melts below 650 °C, shows a significant amount of unreacted MoAlB, as well as evidence for the onset of Mo_2AlB_2 formation. This result suggests that, while the reaction between MoAlB and LiCl occurs much slower than the reaction with $ZnCl_2$, favorable redox pairings of Al with the metal in the metal salt may not be necessary for the transformation to proceed. Finally, NaCl represents a bad redox pair with Al that remains as a solid at 650 °C. No reaction was observed after 1 h, so we allowed the reaction to proceed for 36 h and observed the onset of Mo_2AlB_2 formation, along with significant unreacted MoAlB. As for the LiCl reaction, the NaCl reaction validates that a metal-based redox pair with Al is not needed for Al to be extracted from MoAlB.

Analyzing all four reactions, it is unlikely that metal-based redox reactions, which were invoked for similar reactions of $ZnCl_2$ with the MAX phase Ti_3AlC_2, are operable for the MAB phase MoAlB, since the reaction to form Mo_2AlB_2 proceeds whether or not a redox-active metal pair with Al is present. Also, Al extraction from MoAlB occurs faster when the metal salt with which it reacts is molten, but all reactions proceed regardless of being in the liquid vs. the solid state. These results caused us to consider the role of chloride in helping to facilitate the reaction that transforms MoAlB into Mo_2AlB_2, since the only

commonality among all four metal salt reagents was the chloride counterion. Based on standard reduction potentials, Cl^- would not provide a favorable redox pair with Al; Cl_2 would provide a favorable redox pair with Al, but there is no chemical reaction in our system that would be expected to generate Cl_2. It is well known for MAX phases that in the presence of a halide, the Al that leaves the compound (under conditions that oxidize Al to Al^{3+}) can combine to form aluminum halides, including $AlCl_3$ (with HCl)[17] and AlF_3 (with HF);[18] these halides are rarely observed because they are soluble in the solvents used for synthesis and washing. It is therefore likely that Al oxidizes and combines with Cl^- from the various metal salts in a similar way.

The next consideration, therefore, is how the Al oxidizes. We frequently observe oxide byproducts, including ZnO, Al_2O_3, and MoO_2 (Figures S2 and S4). While the reaction of MoAlB with the metal chlorides occurs under flowing nitrogen, the reaction environment is not rigorously air free, and some oxygen is unavoidably present, including as water vapor from decomposition of the hydrated metal salt reagents. We therefore propose that ambient oxygen is responsible for oxidizing Al to Al^{3+} at the reaction temperature, which is at or above 550 °C. When the reaction between MoAlB and $ZnCl_2$ is carried out in a carbon-coated flame-sealed tube that was more rigorously air-free (except for the water content of $ZnCl_2$, which hydrates even during quick transfer), Mo_2AlB_2 begins to form. However, even after a week it was not phase pure, suggesting that oxygen indeed helps to facilitate the reaction (Figure S6). The presence of Cl^- from the metal salt also provides a reservoir for the Al as it oxidizes to Al^{3+} and exits the MAB phase, while the metal cations from the metal salts combine with oxygen to form the metal oxides that are observed.

For the MAX phase Ti_3AlC_2, the analogous reaction with $ZnCl_2$ at 550 °C produces the exchange product Ti_3ZnC_2. Structural considerations suggest that Al removal without replacement would be unfavorable, as Ti_3AlC_2 already has only a single layer of Al separating the Ti-C layers. For MoAlB, which has a double layer of Al, Al removal (without replacement) leads to the composition $MoAl_{0.5}B$ (*i.e.*, Mo_2AlB_2), which has a single layer of Al and is a metastable phase that is already known to crystallize around 550 °C. Forming Mo_2AlB_2 in the Mo-Al-B system is therefore more favorable than overcoming the barrier of an additional reaction that would require replacing Al with Zn. Conversely, the MAX phase Ti_3AlC_2 is unlikely to accommodate additional Al deficiency, favoring replacement with Zn. Based on these considerations, metal exchange (followed by exfoliation) occurs in the MAX phases while crystallization of a metastable derivative occurs in the MAB phases, under identical conditions.

In conclusion, we have shown that MoAlB reacts with $ZnCl_2$ (and other metal chlorides) to form metastable Mo_2AlB_2, rather than a metal-exchanged product, through a one-step topochemical transformation. This result provides a straightforward alternative to previous routes to Mo_2AlB_2, which is a computationally predicted precursor to a 2-D MBene. It also highlights important differences in chemical reactions applied to MAB phases *vs*. MAX phases.

This material is based upon work supported by the National Science Foundation Graduate Research Fellowship Program under Grant No. DGE1255832. Any opinions, findings, and conclusions or recommendations expressed in this material are those of the authors and do not necessarily reflect the views of the National Science Foundation. This work was also supported by funds from Penn State University. XRD and SEM data were acquired at the Materials Characterization Lab of the Penn State Materials Research Institute. The authors thank Rowan Katzbaer, Lucas Alameda, and James Hodges for insightful discussions and helpful advice.

Conflicts of interest

There are no conflicts to declare.

Notes and references

1 Y. Gogotsi and B. Anasori, *ACS Nano*, 2019, **13**, 8491–8494.
2 B. Anasori, M. R. Lukatskaya and Y. Gogotsi, *Nat. Rev. Mater.*, 2017, **2**, 1–17.
3 M. Li, J. Lu, K. Luo, Y. Li, K. Chang, K. Chen, J. Zhou, J. Rosen, L. Hultman, P. Eklund, P. O. Å. Persson, S. Du, Z. Chai, Z. Huang and Q. Huang, *J. Am. Chem. Soc.*, 2019, **141**, 4730–4737.
4 Z. Guo, J. Zhou and Z. Sun, *J. Mater. Chem. A*, 2017, **5**, 23530–23535.
5 Y. Xiao, Y. Li, Z. Guo, C. Tang, B. Sa, N. Miao, J. Zhou and Z. Sun, *Appl. Surf. Sci.*, 2021, **566**, 150634.
6 J. Jia, B. Li, S. Duan, Z. Cui and H. Gao, *Nanoscale*, 2019, **11**, 20307–20314.
7 R. Li, Y. Liu, H. Deng, C. Yu and Z. Liu, *J. Electrochem. En. Conv. Stor.*, 2020, **17**, 041022.
8 A. Sharma, V. S. Rangra and A. Thakur, *J. Mater. Sci.*, 2022, **57**, 12738–12751.
9 Y. Xiao, C. Shen and T. Long, *Chem. Mater.*, 2021, **33**, 4023–4034.
10 H. Yuan, Z. Li and J. Yang, *J. Phys. Chem. C*, 2019, **123**, 16294–16299.
11 L. T. Alameda, C. F. Holder, J. L. Fenton and R. E. Schaak, *Chem. Mater.*, 2017, **29**, 8953–8957.
12 L. T. Alameda, P. Moradifar, Z. P. Metzger, N. Alem and R. E. Schaak, *J. Am. Chem. Soc.*, 2018, **140**, 8833–8840.
13 K. Kim, C. Chen, D. Nishio-Hamane, M. Okubo and A. Yamada, *Chem. Commun.*, 2019, **55**, 9295–9298.
14 L. T. Alameda, R. W. Lord, J. A. Barr, P. Moradifar, Z. P. Metzger, B. C. Steimle, C. F. Holder, N. Alem, S. B. Sinnott and R. E. Schaak, *J. Am. Chem. Soc.*, 2019, **141**, 10852–10861.
15 Y. Li, H. Shao, Z. Lin, J. Lu, L. Liu, B. Duployer, P. O. Å. Persson, P. Eklund, L. Hultman, M. Li, K. Chen, X.-H. Zha, S. Du, P. Rozier, Z. Chai, E. Raymundo-Piñero, P.-L. Taberna, P. Simon and Q. Huang, *Nat. Mater.*, 2020, **19**, 894–899.
16 W. Jeitschko, *Monatsh. Chem.*, 1966, **97**, 1472–1476.
17 C. Wang, H. Shou, S. Chen, S. Wei, Y. Lin, P. Zhang, Z. Liu, K. Zhu, X. Guo, X. Wu, P. M. Ajayan and L. Song, *Adv. Mater.*, 2021, **33**, 2101015.
18 P. Srivastava, A. Mishra, H. Mizuseki, K.-R. Lee and A. K. Singh, *ACS Appl. Mater. Interfaces*, 2016, **8**, 24256–24264.

